observed. The analysis described here is particularly important in that it demonstrates which flow parameters are most suitable for the correlation of experimental data and allow standoff distances to be estimated quickly without the need to run time-consuming computational fluid dynamics codes, though such codes should be used to provide more detailed information where required.

## Acknowledgments

The authors wish to thank H. Ojima and T. Ogawa for their assistance in conducting the experimental work described in the paper by Nonaka et al. (Nonaka, S., Mizuno, H., and Takayama, K., "Ballistic Range Measurement of Shock Shapes in Intermediate Hypersonic Regime," AIAA Paper 99-1025, Jan. 1999).

## References

[1]Hornung, H. G., "Non-Equilibrium Dissociating Nitrogen Flow over Spheres and Circular Cylinders," *Journal of Fluid Mechanics*, Vol. 53, 1972, pp. 149–176.

[2]Hornung, H. G., and Wen, C.-Y., "Non-Equilibrium Dissociating Flows over Spheres," AIAA Paper 95-0091, Jan. 1995.

[3]Vincenti, W. G., and Kruger, C. H., *Introduction to Physical Gas Dynamics*, Wiley, New York, 1965, pp. 198–206.

[4]Millikan, R. C., and White, D. R., "Systematics of Vibrational Relaxation," *Journal of Chemical Physics*, Vol. 39, No. 12, 1963, pp. 3209–3213.

[5]Park, C., *Non-Equilibrium Hypersonic Aerothermodynamics*, Wiley, New York, 1990, pp. 56–60.

[6]Nonaka, S., Mizuno, H., and Takayama, K., "Ballistic Range Measurement of Shock Shapes in Intermediate Hypersonic Regime," AIAA Paper 99-1025, Jan. 1999.

M. Sichel
*Associte Editor*

# Centerline Vorticity Transport Within a Jet in Crossflow

Václav Kolář*
*Institute of Hydrodynamics,*
*166 12 Prague 6, Czech Republic*
and
Eric Savory† and Norman Toy‡
*University of Surrey,*
*Guildford, England GU2 5XH, United Kingdom*

## Introduction

THE single circular jet issuing normally into a crossflow (JICF) represents one of the basic jet-flow configurations with a wide variety of practical applications. These range from the aerodynamics of advanced short takeoff and landing (ASTOVL) aircraft and jet steering systems, through combustion chamber mixing, to environmental flows. Margason[1] provides an extensive survey of JICF studies during the past 50 years up to 1993 and recent papers, e.g., Smith and Mungal,[2] have shed a new light on the JICF problem as well. Though many aspects of the JICF including vorticity distributions (e.g., Refs. 3 and 4) have been treated in the literature, some aspects, such as the turbulent vorticity transport and the associated vortex strength decay of the well-known contrarotating vortex pair (CVP), still need to be clarified.

The aim of the present contribution has been to carry out the measurement of velocity fields and turbulence statistics in such a manner as to be able to visualize the centerline vorticity transport across the plane of symmetry (which is supposed to be the main cause of the cancellation of the vortex strength of the CVP) and to analyze the corresponding circulation decay rate directly in terms of the Reynolds stresses. Decay rates are closely associated with the effective turbulent vorticity fluxes defined in a manner similar to that in previous work[5] and determined by an analogous method as introduced by Kolář[6] for the planar case.

It is well recognized that large-scale organized vortical structures may exist within the flow field.[7] However, in the present work these are not taken into account and are reflected only as an inherent contribution to the long-time-averaged values of relevant quantities (denoted by angular brackets $\langle \cdots \rangle$).

## Experimental Details

The measurements were carried out in a wind tunnel in the Department of Civil Engineering at the University of Surrey, using the standard crossed hot-wire anemometry technique. The tunnel working cross section was 0.62 m wide $\times$ 0.75 m high, and the jet nozzle of diameter $D = 13$ mm was placed flush with the ground plane. The jet outlet velocity was $U_J = 53.0$ m/s, resulting in $Re_J \approx 4.6 \times 10^4$. Only one jet-velocity/crossflow-velocity ratio, $R = U_J/U_C$, was studied, namely the ratio $R = 8$. Hence, the crossflow velocity was set to be $U_C = 6.63$ m/s. Flow symmetry is assumed in order to reduce the range of measurements to a half-plane. The coordinate system is shown in Fig. 1 with the origin at the center of the jet exit.

The crossed hot-wire measurements were, whenever necessary, undertaken with a tilted probe that was approximately aligned with the preestimated mean flow direction and the Reynolds stresses of interest were reconstructed based on the decompositions in the manner of Cutler and Bradshaw[8] using four probe roll positions. In the present case there is no wall effect and the probe volume is relatively small in comparison with the flow structures being investigated. Hence, the gradient errors will be within the bounds found previously.[8]

The velocity fields, that is the projections of the velocity vectors, $(\langle u \rangle, \langle v \rangle, \langle w \rangle)$, in the planes $x = $Const., were determined in five equidistant rectangular cross sections located at $x/D = 10$, 12.5, 15, 17.5, and 20 with dimensions $z = 70$–$250$ mm ($z/D \approx$ 5.4–19.2), $y = 0$–$100$ mm ($y/D \approx 0$–$7.7$), and with a square measurement mesh having steps of 10 mm. In the four corresponding midplanes, some necessary additional measurements of Reynolds stress tensor components in the centerline region were taken as well.

## Turbulent Vorticity Fluxes

The only vorticity component considered here is the dominant one, aligned with the crossflow direction $x$, denoted $\langle \omega \rangle$. Figure 2a shows $\langle \omega \rangle$ for the measured half of the CVP for $x/D = 15$ ($x/RD = 1.875$). The coordinate $RD$-scaling, adopted in Figs. 2 and 3, has been found as the most appropriate scaling for physical dimensions of the JICF.[2]

Following previous work,[5] the turbulent transport of the mean vorticity is characterized by the antisymmetric turbulent vorticity flux-density tensor, which can be expressed purely in terms of gradients of the Reynolds stress tensor components. Along the centerline there is only one generally nonzero component of turbulent vorticity flux-density *vector* associated with $\langle \omega \rangle$, namely the $y$ component, which is responsible for the centerline vorticity exchange between the single vortices of the CVP. The $y$ component of the so-called *effective*[5] (that is, having generally a nonzero effect on $\mathrm{D}\langle \omega \rangle / \mathrm{D}t$

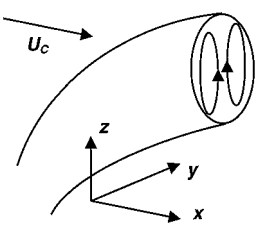


**Fig. 1 Coordinate system.**

Received 1 October 1999; revision received 28 April 2000; accepted for publication 1 May 2000. 

*Senior Researcher, Academy of Sciences.

†Lecturer, Fluid Mechanics Research Group, Department of Civil Engineering.

‡Professor, Fluid Mechanics Research Group, Department of Civil Engineering.

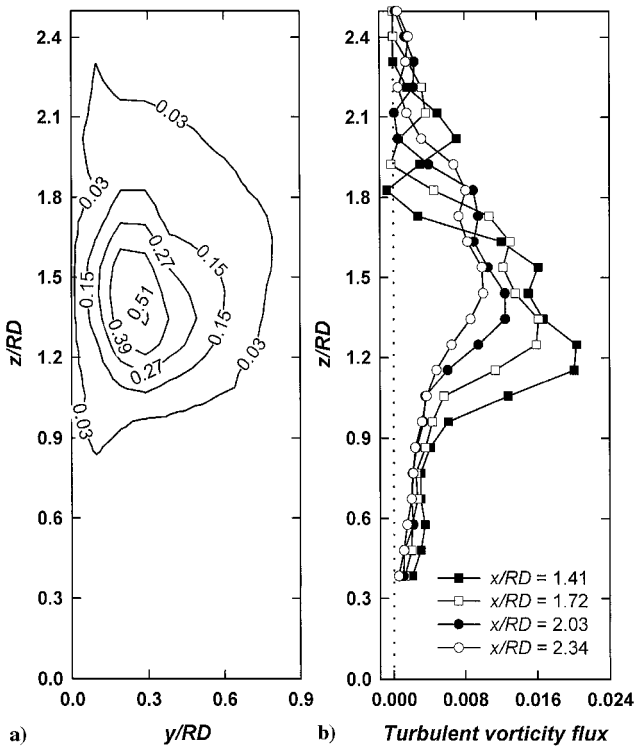


**Fig. 2 a) Normalized negative vorticity, $-\omega D/U_C$ for $x/D = 15$ ($x/RD = 1.875$). b) Effective turbulent vorticity flux (reduced, normalized by $U_C^2/D$).**

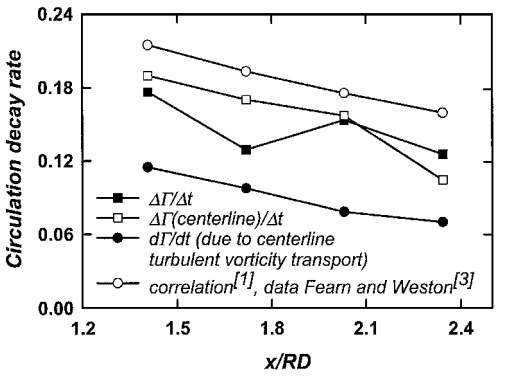


**Fig. 3 Circulation decay rate in downstream direction (normalized by $U_C^2$).**

in the mean vorticity transport equation) turbulent vorticity flux-density vector of $\langle\omega\rangle$ reads

$$J^y = (\langle w'^2\rangle - \langle v'^2\rangle)_z/2 + \langle v'w'\rangle_y + \langle u'w'\rangle_x \qquad (1)$$

(The subscripts stand for partial derivatives, and the superscript $y$ denotes the vector component.)

The first flux term on the right-hand side of Eq. (1) dealing with normal Reynolds stresses does not contribute to the circulation decay, as will be discussed in the next section, and may be neglected. Figure 2b shows reduced flux distributions for the four midplanes (with respect to five cross sections of the measured velocity vector plots), namely, for $x/D = 11.25, 13.75, 16.25$, and $18.75$ ($x/RD = 1.41, 1.72, 2.03$, and $2.34$). The flux distributions indicate that the peak values of the turbulent vorticity transport across the centerline can be found close to the $z$ location of the vorticity and upwash ($\langle w\rangle$ component) velocity peaks. The natural downstream decrease of vorticity transport is observed from the decrease in the flux values. A small upward $z$ shift also occurs, which is due to the lifting of the jet trajectory. An interesting local minimum of the vorticity flux, due to the negative minimum of the last flux term in Eq. (1), can be recognized close to the position of the maximum of the centerline streamwise velocity.

## Circulation Decay Rate

Direct estimates of the circulation decay rate, denoted as $\Delta\Gamma/\Delta t$, may be inferred directly from two consecutive streamwise cross sections with the time difference estimated from the crossflow velocity $U_C$ and the $x$ difference between two consecutive planes. For simplicity, the whole measurement region is used for calculating $\Gamma$ as a surface quadrature of $\langle\omega\rangle$.

The circulation decay rate $\mathrm{d}\Gamma/\mathrm{d}t$ is described in terms of fluxes by

$$\frac{\mathrm{d}\Gamma}{\mathrm{d}t} = -\int_A \left(J_y^y + J_z^z\right)\mathrm{d}A = \oint_C (J^y\,\mathrm{d}z - J^z\,\mathrm{d}y) \qquad (2)$$

where $C$ is a vortex boundary. This expression can be derived analogously as for planar case[6] where the kinematics of surface integrals[9] is applied to the vorticity vector, namely, the key formula for

$$\frac{\mathrm{d}}{\mathrm{d}t}\int_A \langle\omega\rangle\cdot\boldsymbol{n}\,\mathrm{d}A$$

is employed and substituted from the vorticity transport equation in divergence form[5] so the contribution of the tilting-and-stretching term cancels out.

The estimates of $\mathrm{d}\Gamma/\mathrm{d}t$ due to centerline turbulent vorticity transport are derived simply by integration of $J^y\,\mathrm{d}z$ over the relevant centerline interval $I$ (for simplicity, the whole centerline velocity measurement interval $z = 70$–$250$ mm, or $z/D \approx 5.4$–$19.2$, is used for calculation):

$$\left(\frac{\mathrm{d}\Gamma}{\mathrm{d}t}\right)_{\text{centerline vorticity transport}} = \int_I J^y\,\mathrm{d}z = \int_I (\langle v'w'\rangle_y + \langle u'w'\rangle_x)\,\mathrm{d}z \qquad (3)$$

where $J^y$ is given by Eq. (1), reduced a priori in the first term. This reduction is possible provided that the integration limits are placed in the low turbulence regions outside the CVP. It should be recalled that the total circulation decay rate due to turbulence is given by Eq. (2).

Figure 3 shows the comparison between the direct estimates $\Delta\Gamma/\Delta t$, and the estimated values of $\mathrm{d}\Gamma/\mathrm{d}t$ due to the centerline turbulent vorticity transport, calculated from Eq. (3). The values of $\Delta\Gamma/\Delta t$ inferred from the "universal" correlation in Margason[1] (see Fig. 23b taken from his Ref. 13, Smy and Ransom, 1976) based on data from Fearn and Weston,[3] are shown for comparison as well. Further, the figure includes the decay rate derived from the change in the centerline line-integral of the upwash velocity. Some preliminary analysis of the present data and others[10] indicates that the dominant portion of vortex circulation can be obtained as a mere centerline line-integral of the upwash velocity $\langle w\rangle$, and the centerline circulation decay rate, calculated from the centerline upwash velocity data at two consecutive cross sections downstream, can be taken as quasi-Galilean invariant.

The results indicate that the rate of change in the centerline line-integral of the upwash velocity corresponds quite well to the direct estimates of $\Delta\Gamma/\Delta t$ as calculated from $\langle\omega\rangle$ fields. The estimates of $\mathrm{d}\Gamma/\mathrm{d}t$ based on the centerline turbulence statistics, see (3), attain, on average, two thirds of the directly estimated total decay rate $\Delta\Gamma/\Delta t$. The resulting effect upon $\mathrm{d}\Gamma/\mathrm{d}t$ of the second flux term in Eq. (1) is an order of magnitude higher than that of the third one.

## Conclusions

The crucial role of centerline vorticity transport responsible for the cancellation of the vortex strength of the CVP within the JICF has been visualized in terms of effective turbulent vorticity fluxes and the associated circulation decay has been analyzed. The circulation decay rate due to turbulent vorticity transport depends merely upon the turbulence properties (of anisotropy and inhomogeneity of Reynolds stresses) at the vortex contour, a significant part of which is just the centerline "separating" the single vortices of the CVP.

## Acknowledgments

V. Kolář gratefully acknowledges the support of the Royal Society (U.K.) and the University of Surrey during his stay in the United

Kingdom, together with the support of the GA Academy of Sciences of the Czech Republic through Grant A2060803. Thanks are also due to S. McCusker for his kind assistance with the experimental work.

## References

[1]Margason, R. J., " Fifty Years of Jet in Crossflow Research," CP-534, AGARD, Nov. 1993, pp. 1.1–1.41.

[2]Smith, S. H., and Mungal, M. G., "Mixing, Structure and Scaling of the Jet in Crossflow," *Journal of Fluid Mechanics*, Vol. 357, 1998, pp. 83–122.

[3]Fearn, R., and Weston, R. P., "Vorticity Associated with a Jet in a Cross Flow," *AIAA Journal*, Vol. 12, No. 12, 1974, pp. 1666–1671.

[4]Sykes, R. I., Lewellen, W. S., and Parker, S. F., "On the Vorticity Dynamics of a Turbulent Jet in a Crossflow," *Journal of Fluid Mechanics*, Vol. 168, 1986, pp. 393–413.

[5]Kolář, V., Lyn, D. A., and Rodi, W., "Ensemble-Averaged Measurements in the Turbulent Near Wake of Two Side-by-Side Square Cylinders," *Journal of Fluid Mechanics*, Vol. 346, 1997, pp. 201–237.

[6]Kolář, V., "Decay Rates of Coherent Structures in a Plane Turbulent Wake," *Proceedings of 13th Australasian Fluid Mechanics Conference*, edited by M. C. Thompson and K. Hourigan, Vol. 2, Monash Univ., Melbourne, Australia, 1998, pp. 721–725.

[7]Papaspyros, J. N. E., Kastrinakis, E. G., and Nychas, S. G., "Coherent Contribution to Turbulent Mixing of a Jet in Cross Flow," *Applied Scientific Research*, Vol. 57, No. 3–4, 1997, pp. 291–307.

[8]Cutler, A. D., and Bradshaw, P., "A Crossed Hot-Wire Technique for Complex Turbulent Flows," *Experiments in Fluids*, Vol. 12, No. 1–2, 1991, pp. 17–22.

[9]Truesdell, C., and Toupin, R. A., "The Classical Field Theories," *Encyclopedia of Physics*, edited by S. Flügge, Vol. 3/1, Principles of Classical Mechanics and Field Theory, Springer-Verlag, Berlin, 1960, p. 346.

[10]Savory, E., Toy, N., and Ahmed, S., "Experimental Study of a Plume in a Crossflow," *Journal of Wind Engineering and Industrial Aerodynamics*, Vol. 60, No. 1–3, 1996, pp. 195–209.

J. P. Gore
*Associate Editor*

# Roughness and Turbulence Effects on the Surface Pressure over Yawed Cylinders

A. Gatto,* N. A. Ahmed,† and R. D. Archer‡
*University of New South Wales, Sydney, New South Wales 2052, Australia*

## Nomenclature

$AR$ = aspect ratio measured perpendicular to airstream
$B$ = blockage ratio
$Cp$ = coefficient of pressure $(P - P_\infty)/q$
$d$ = outer diameter of cylinder
$k$ = roughness height
$q$ = freestream dynamic pressure
$Re_n$ = Reynolds number based on cylinder diameter and freestream velocity
$Tu$ = turbulence intensity
$\theta$ = circumferential angular position from stagnation position
$\Lambda$ = yaw angle

## Introduction

THE effects of freestream turbulence and surface roughness on mean and fluctuating surface pressures over a circular cylinder placed perpendicular to the airstream is an active research area in modern aerodynamics.[1,2] Of particular interest is the resulting nature of the flow over a yawed circular cylinder when such secondary effects are applied. This Note documents tests over smooth and rough 45-deg yawed circular cylinders in both smooth and turbulent freestreams. Results from investigations show that mean pressure over the model in all configurations established infinitely long circular cylinder conditions over part of the span. Results from fluctuating pressure distributions, however, showed no sign of infinitely long circular cylinder conditions except in a turbulent freestream. The increased ability of the turbulent freestream to generate infinitely long circular cylinder conditions is thought to be due to the increased mixing and entrainment with which a turbulent freestream imparts to the separating shear layers, reducing the effect of the exposed free end. Results from the roughened model showed highly asymmetric fluctuating pressure distributions, further indicating that both the mean and fluctuating pressures should be considered if infinitely long circular cylinder conditions are required.

## Experimental Arrangement and Procedure

All tests were conducted in an open-circuit, closed-test-section, low-turbulence (0.2% at 40 m/s) wind tunnel on yawed circular-cylinder models at a Reynolds number of $9.6 \times 10^4$. Three flow configurations were analyzed: a smooth model ($k/d < 10^{-5}$) in low freestream turbulence (denoted as *smooth*), a smooth model in grid-generated turbulence (denoted as *turbulent*), and a roughened model in low freestream turbulence (denoted as *rough*). To simulate the turbulent flowfield, a square-mesh, biplanar, turbulence-generating grid was placed between the outlet of the contraction and the entrance to the test section. The grid was composed of circular cross-section rods 2.5 mm in diameter and spaced at 25-mm intervals. The longitudinal turbulence intensity and integral length scale for this flow configuration were measured at the model station using a hot-wire anemometer at 2% and 14 mm, respectively. The upstream end of the model was 12 mesh spacings downstream from the meshed grid, ensuring that the model was in homogeneous turbulence.[3] Roughness was simulated by covering the entire span of the model with Norton 60-grit emery paper. Holes of 1-mm diameter were carefully punched into the emery paper to coincide with the pressure tap holes in the model. The relative roughness of the paper was estimated to be $k/d = 500 \times 10^{-5}$.

The yawed circular cylinder basic model configuration is shown in Fig. 1. The models spanned the 457 × 457 mm test section and were mounted 30 mm off the tunnel walls using support blocks. The test section blockage ratio $B$ and model aspect ratio $AR$ (measured perpendicular to the airstream) were kept constant for all configurations at 10% and 10, respectively. Having these conditions for

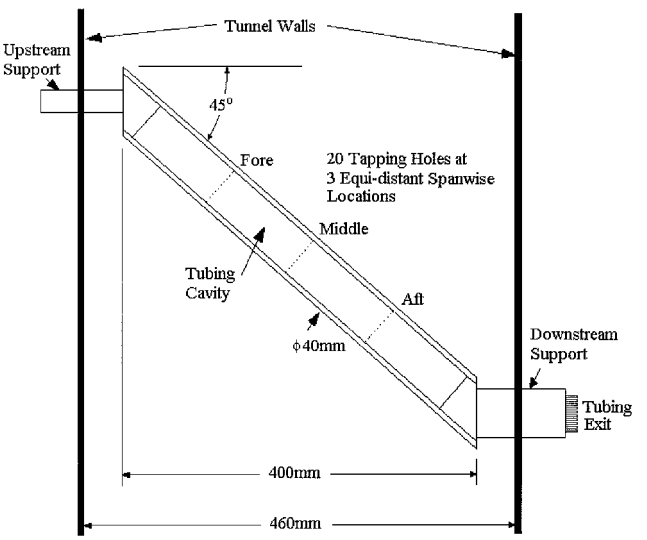


**Fig. 1 A 45-deg yawed circular cylinder: flow direction, top to bottom of page.**

Received 14 December 1999; revision received 23 February 2000; accepted for publication 2 March 2000. 

*Research Assistant, School of Mechanical and Manufacturing Engineering.
†Senior Lecturer, School of Mechanical and Manufacturing Engineering.
‡Professor, School of Mechanical and Manufacturing Engineering. Senior Member AIAA.